Inorg. Chem. **2007**, *46*, 5911–5921

A QM/MM Investigation of the Activation and Catalytic Mechanism of Fe-Only Hydrogenases

Claudio Greco,[†,‡] Maurizio Bruschi,[§] Luca De Gioia,*[,†] and Ulf Ryde*[,‡]

Department of Biotechnology and Biosciences, University of Milano-Bicocca, Piazza della Scienza 2, 20126 Milano, Italy, Department of Theoretical Chemistry, Lund University, P.O. Box 124, Lund S-221 00, Sweden, and Department of Environmental Sciences, University of Milano-Bicocca, Piazza della Scienza 1, 20126 Milano, Italy

Received December 5, 2006

Fe-only hydrogenases are enzymes that catalyze dihydrogen production or oxidation, due to the presence of an unusual Fe_6S_6 cluster (the so-called H-cluster) in their active site, which is composed of a Fe_2S_2 subsite, directly involved in catalysis, and a classical Fe_4S_4 cubane cluster. Here, we present a hybrid quantum mechanical and molecular mechanical (QM/MM) investigation of the Fe-only hydrogenase from *Desulfovibrio desulfuricans*, in order to unravel key issues regarding the activation of the enzyme from its completely oxidized inactive state ($\mathbf{H_{ox}^{inact}}$) and the influence of the protein environment on the structural and catalytic properties of the H-cluster. Our results show that the Fe_2S_2 subcluster in the $Fe^{II}Fe^{II}$ redox state—which is experimentally observed for the completely oxidized form of the enzyme—binds a water molecule to one of its metal centers. The computed QM/MM energy values for water binding to the diferrous subsite are in fact over 70 kJ mol^{-1}; however, the affinity toward water decreases by 1 order of magnitude after a one-electron reduction of $\mathbf{H_{ox}^{inact}}$, thus leading to the release of coordinated water from the H-cluster. The investigation of a catalytic cycle of the Fe-only hydrogenase that implies formation of a terminal hydride ion and a di(thiomethyl)amine (DTMA) molecule acting as an acid/base catalyst indicates that all steps have reasonable reaction energies and that the influence of the protein on the thermodynamic profile of H_2 production catalysis is not negligible. QM/MM results show that the interactions between the Fe_2S_2 subsite and the protein environment could give place to structural rearrangements of the H-cluster functional for catalysis, provided that the bidentate ligand that bridges the iron atoms in the binuclear subsite is actually a DTMA residue.

1. Introduction

Fe-only hydrogenases are enzymes that catalyze the reversible oxidation of molecular hydrogen and are expressed by a large variety of anaerobic microorganisms able to use protons as electron acceptors for their redox metabolism.[1] In particular, Fe-only hydrogenases are very efficient as hydrogen-evolving enzymes in vivo,[2] attracting the attention of theoretical and experimental chemists interested in understanding the basis of the catalytic efficiency[3] and in reproducing it in synthetic assemblies.[4]

The active site of Fe-only hydrogenases consists of a peculiar Fe_6S_6 iron−sulfur cluster, referred to as the "H-cluster", which is composed of a classic Fe_4S_4 cluster and a Fe_2S_2 subsite that is directly involved in catalysis (Scheme 1).[5] The two subclusters are bridged by the sulfur atom of a cysteine residue. The coordination environment of the iron

* To whom correspondence should be addressed. E-mail: luca.degioia@unimib.it (L.D.G), ulf.ryde@teokem.lu.se (U.R.). Tel: +46-46-22245 02 (U.R.). Fax: +39-02-64483478 (L.D.G.), +46-46-22245 43 (U.R.).

† Department of Biotechnology and Biosciences, University of Milano-Bicocca.

‡ Department of Theoretical Chemistry, Lund University.

§ Department of Environmental Sciences, University of Milano-Bicocca.

(1) Adams, M. W. W. *Biochim. Biophys. Acta* **1990**, *1020*, 115−145. Cammack, R. *Nature* **1999**, *397*, 214−215. Nicolet, Y.; Lemon, B. J.; Fontecilla-Camps, J. C.; Peters, J. W. *Trends Biochem. Sci.* **2000**, *25*, 138−143. Peters, J. W. *Curr. Opin. Struct. Biol.* **1999**, *9*, 670−676. Horner, D. S.; Heil, B.; Happe, T.; Embley, T. M. *Trends Biochem. Sci.* **2002**, *27*, 148−153. Nicolet, Y.; Cavazza, C.; Fontecilla-Camps, J. C. *J. Inorg. Biochem.* **2002**, *91*, 1−8. *Hydrogen as Fuel—Learning from Nature*; Cammack, R., Frey, M., Robson, R., Eds.; Taylor and Francis: London, 2001. Armstrong, F. A. *Curr. Opin. Chem. Biol.* **2004**, *8*, 133−140.

(2) Frey, M. *Chembiochem* **2002**, *3*, 153−160.

(3) Bruschi, M.; Zampella, G.; Fantucci, P.; De Gioia, L. *Coord. Chem. Rev.* **2005**, *15−16*, 1620−1640.

(4) Liu, X.; Ibrahim, S. K.; Tard, C.; Pickett, C. J. *Coord. Chem. Rev.* **2005**, *15−16*, 1641−1652.

10.1021/ic062320a CCC: $37.00
Published on Web 06/29/2007

Scheme 1. Structure of Fe-Only Hydrogenase Binuclear Subsite as Observed through X-ray Diffraction (left side);[5b] the Geometry of the Synthetic Complex (μ-PDT)[Fe(CO)$_3$]$_2$ (right side)

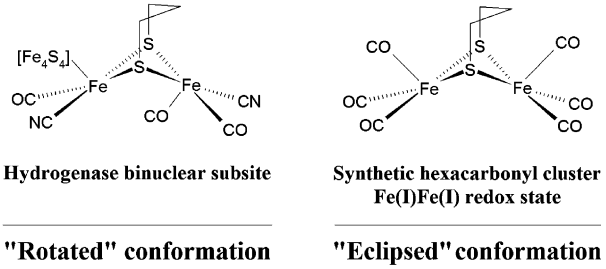

Scheme 2. $\mathbf{H_{ox}^{inact}}$ Form of the H-cluster[a]

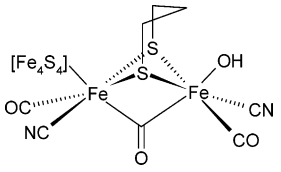

[a] As proposed by Liu and Hu.[10b]

atoms in the binuclear subsite is completed by three CO and two CN^- ligands and by a bridging ligand of formula S−X_3−S, which has been proposed to correspond to propanedithiolate (PDT) or di(thiomethyl)amine (DTMA).[5,6] The two iron atoms of the Fe_2S_2 subsite are commonly referred to as "proximal" (Fe_p) and "distal" (Fe_d), depending on their position with respect to the Fe_4S_4 subcluster.

Experimental[7−9] and computational[10] investigations suggest that the binuclear subsite can attain at least three different redox states: $Fe^{II}Fe^{II}$ for the completely oxidized, catalytically inactive form of the enzyme ($\mathbf{H_{ox}^{inact}}$), in which a H_2O or a hydroxo group could be bound to the Fe_2S_2 subsite (Scheme 2), $Fe^{II}Fe^{I}$ for the partially oxidized, active state of the biocatalyst ($\mathbf{H_{ox}^{cat}}$), and $Fe^{I}Fe^{I}$ for the reduced form of the protein ($\mathbf{H_{red}}$). Notably, the Fe_4S_4 subsite has the same redox state ($[Fe_4S_4]^{2+}$) in the three forms of the protein.[9f] Moreover, redox titrations showed that the $\mathbf{H_{ox}^{inact}}$ form initially converts, in a reversible one-electron step, to a so-called $\mathbf{H_{trans}}$ form, which converts irreversibly into the $\mathbf{H_{ox}^{cat}}$ state in a step most likely involving two electrons, which do not end up on Fe atoms of the H-cluster.[11] In addition to the H-cluster, Fe-only hydrogenases also contain other iron−sulfur assemblies; for example, the X-ray crystal structure of the hydrogenase from *Desulfovibrio desulfuricans* (DdH) showed that it contains two accessory Fe_4S_4 clusters.[6]

Besides the X-ray structure of DdH, additional crystal structures of Fe-only hydrogenases are currently available, viz., the enzyme from *Clostridium pasteurianum* (CpI), both in its carbon monoxide inhibited form,[12] which bears an additional CO group bound to Fe_d, and in an oxidized form showing a solvent molecule coordinated to the same iron center.[5a,12] Unfortunately, it has in no case been possible to unambiguously assign the redox state of the H-cluster in the crystals.

To date, several alternative hypotheses for the catalytic cycle of Fe-only hydrogenases have been investigated. Some studies[13] have explored pathways in which a hydride group bridging the two iron ions of the binuclear subsite could play a role in catalysis. However, it was noted that the DTMA ligand could conveniently act as an acid/base during catalysis.[5b] Starting from this assumption, Liu and Hu and Fan and Hall[10b,14] have reported, on the basis of QM investigations of binuclear models, that a catalytic cycle involving two proton-transfer reactions from DTMA to the distal iron ion, each followed by a one-electron reduction, provides a facile path for hydrogen production or oxidation (see Scheme 3).[10b,14,15] Such a mechanism involves the formation of terminal hydride adducts, and notably, recent experimental data on the biomimetic complex $[Fe_2(S_2C_2H_4)(\mu\text{-CO})(H)(CO)(PMe_3)_4]^+$ showed that a terminal hydride can be more reactive than a bridging hydride.[16]

The formation of a terminal hydride during catalysis is also supported by the crystal structure of the reduced Fe-only hydrogenase from *D. desulfuricans*,[5b] which shows that the binuclear subcluster features a semibridging carbonyl ligand. Moreover, the coordination position trans to the μ-CO group on Fe_d is apparently vacant. Such a geometry of the H-cluster—referred to as the "rotated" conformation, as opposed to an "eclipsed" conformation characterized by all terminal ligands, see Scheme 1—is expected to favor the formation of a terminal hydride species. There is no experimental evidence of the possibility that the H-cluster binuclear subsite can reside in an eclipsed conformation in

(5) (a) Peters, J. W.; Lanzilotta, W. N.; Lemon, B. J.; Seefeldt, L. C. *Science* **1998**, *282*, 1853−1858. (b) Nicolet, Y.; de Lacey, A. L.; Vernede, X.; Fernandez, V. M.; Hatchikian, E. C.; Fontecilla-Camps, J. C. *J. Am. Chem. Soc.* **2001**, *123*, 1596−1601.
(6) Nicolet, Y.; Piras, C.; Legrand, P.; Hatchikian, E. C.; Fontecilla-Camps, J. C. *Structure* **1999**, *7*, 13−23.
(7) Lyon, E. J.; Georgakaki, I. P.; Reibenspies, J. H.; Darensbourg, M. Y. *Angew. Chem., Int. Ed.* **1999**, *38*, 3178−3180. Rauchfuss, T. B.; Contakes, S. M.; Schmidt, M. *J. Am. Chem. Soc.* **1999**, *121*, 9736−9737. Cloirec, A. L.; Best, S. P.; Borg, S.; Davies, S. C.; Evans, D. J.; Hughes, D. L.; Pickett, C. J. *Chem. Commun.* **1999**, 2285−2286. Lai, C.-H.; Lee, W.-Z.; Miller, M. L.; Reibenspies, J. H.; Darensbourg, D. J.; Darensbourg, M. Y. *J. Am. Chem. Soc.* **1998**, *120*, 10103−10114.
(8) Evans, D. J.; Pickett, C. J. *Chem. Soc. Rev.* **2003**, *35*, 268−275. Rauchfuss, T. B. *Inorg. Chem.* **2004**, *43*, 14−26. Chen, Z.; Lemon, B. J.; Huang, S.; Swartz, D. J.; Peters, J. W.; Bagley, K. A. *Biochemistry* **2002**, *41*, 2036−2043.
(9) (a) Adams, M. W. W.; Mortenson, L. E. *J. Biol. Chem.* **1984**, *259*, 7045−7055. (b) Adams, M. W. W. *J. Biol. Chem.* **1987**, *262*, 15054−15061. (c) Zambrano, I. C.; Kowal, A. T.; Mortenson, L. E.; Adams, M. W. W.; Johnson, M. K. *J. Biol. Chem.* **1989**, *264*, 20974−20983. (d) Pierik, A. J.; Hagen, W. R.; Redeker, J. S.; Wolbert, R. B. G.; Boersma, M.; Verhagen, M. F.; Grande, H. J.; Veeger, C.; Mustsaers, P. H. A.; Sand, R. H.; Dunham, W. R. *Eur. J. Biochem.* **1992**, *209*, 63−72. (e) Rusnak, F. M.; Adams, M. W. W.; Mortenson, L. E.; Munck, E. *J. Biol. Chem.* **1987**, *262*, 38−41. (f) Popescu, C. V.; Munck, E. *J. Am. Chem. Soc.* **1999**, *121*, 7877−7884.
(10) (a) Cao, Z.; Hall, M. B. *J. Am. Chem. Soc.* **2001**, *123*, 3734−3742. (b) Liu, Z.-P.; Hu, P. *J. Am. Chem. Soc.* **2002**, *124*, 5175−5182.
(11) (a) Roseboom, W.; De Lacey, A. L.; Fernandez, V. M.; Hatchikian, E. C.; Albracht, S. P. J. *J. Biol. Inorg. Chem.* **2006**, *11*, 102−118. (b) Pereira, A. S.; Tavares, P.; Moura, I.; Moura, J. J.; Huynh, B. H. *J. Am. Chem. Soc.* **2001**, *123*, 2771−2782.
(12) Lemon, B. J.; Peters, J. W. *Biochemistry* **1998**, *38*, 12969−12973.
(13) Bruschi, M.; Fantucci, P.; De Gioia, L. *Inorg. Chem.* **2002**, *41*, 1421. Bruschi, M.; Fantucci, P.; De Gioia, L. *Inorg. Chem.* **2003**, *42*, 4773−4781. Zhou, T.; Mo, Y.; Liu, A.; Zhou, Z.; Tsai, K. R. *Inorg. Chem.* **2004**, *43*, 923−930.
(14) Fan, H.-J.; Hall, M. B. *J. Am. Chem. Soc.* **2001**, *123*, 3828−3829.
(15) Zampella, G.; Greco, C.; Fantucci, P.; De Gioia, L. *Inorg. Chem.* **2006**, *45*, 4109−4118.
(16) van der Vlugt, J. I.; Rauchfuss, T. B.; Whaley, C. M.; Wilson, S. R. *J. Am. Chem. Soc.* **2005**; *127*, 16012−16013.

Scheme 3. Steps of a Hypothetical Hydrogen-Evolving Path That Should Be Associated with a Favorable Energy Profile, Both at the Kinetic and Thermodynamic Levels[a]

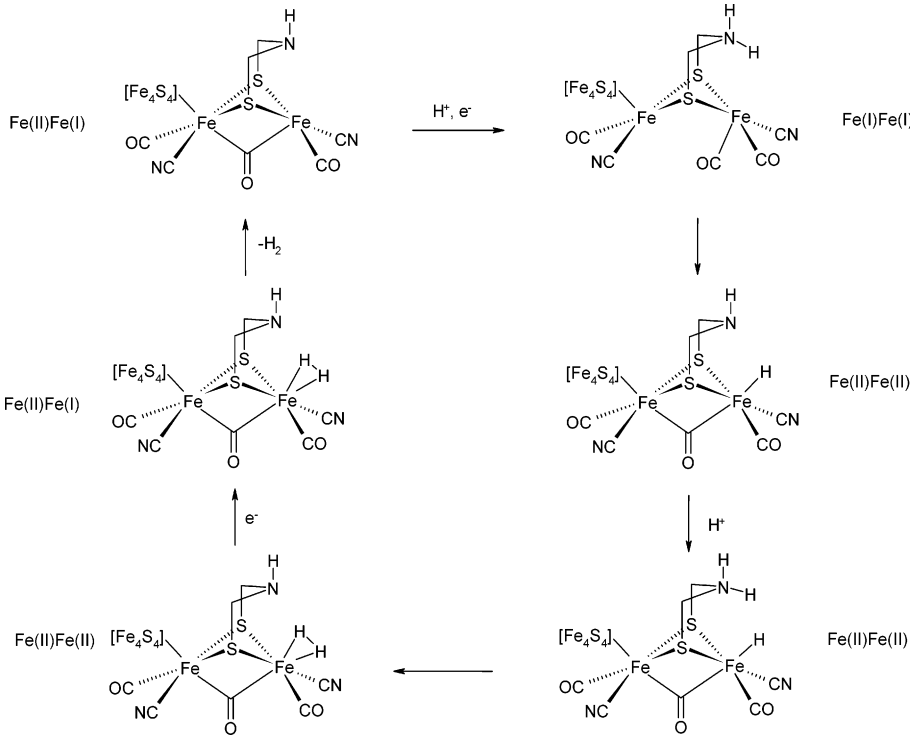

[a] This scheme summarizes the DFT results obtained by Liu and Hu,[10b] Fan and Hall,[14] and Zampella et al.[15] on DFT models of Fe-only hydrogenase binuclear subsites.

physiological conditions. However, it is important to note that all biomimetic di-iron clusters synthesized so far, which are catalytically far less efficient than the enzyme, are invariably in the eclipsed conformation (see Scheme 1)[17] and their protonation leads to bridging hydride adducts.[18] Therefore, it is of great relevance for the design of efficient biomimetic catalysts to understand if the peculiar structure of the H-cluster depends only on the stereoelectronic properties of the atoms forming the cluster or if the protein environment plays a role affecting its structural and electronic properties. More generally speaking, the influence of the protein environment on the structure and reactivity of the Fe_6S_6 cluster is largely unknown.

Prompted by the above observations, we have carried out a combined quantum mechanical and molecular mechanical (QM/MM) investigation of the activation and catalytic mechanism of the Fe-only hydrogenase from *D. desulfuricans*, treating the whole Fe_6S_6 cluster at QM level, using the broken-symmetry (BS) approximation.[19] First, we have studied the activation of the enzyme from its $\mathbf{H_{ox}^{inact}}$ form, considering three different forms of the $Fe^{II}Fe^{II}$ binuclear subcluster: a rotated form showing a vacant coordination site trans to the bridging CO, a hydroxo-bound form, and a water-bound form. Both DTMA and PDT have been considered as plausible bidentate ligands of the di-iron subsite. The effects of one-electron reduction on the structure of the hydroxo- and water-bound Fe_2S_2 subcluster were also investigated. Then, we have investigated the most plausible catalytic mechanism of Fe-only hydrogenases, in which the amine group of DTMA acts as an acid/base group during the proton-transfer reactions, to highlight possible roles played by the protein environment.

2. Computational Details

2.1. QM/MM Approach. All QM/MM optimizations were carried out with the *COMQUM* program suite.[20,21] In the current version, it uses *Turbomole 5.7*[22] for the QM part and *Amber 8*[23] (with the 1999 force field[24]) for the MM part. In such a hybrid approach, the protein and solvent are divided into three subsystems: System 1 is treated at the QM level and contains the H-cluster atoms and relevant surrounding atoms (see below). System 2 consists of all residues with any atom within 12 Å of any atom in system 1, and it is optimized by a full MM minimization in each step of the QM/MM energy minimization. Finally, the remaining portion of the protein, together with the water molecules

(17) Tye, J. W.; Darensbourg, M. Y.; Hall, M. B. *Inorg. Chem.* **2006**, *45*, 1552−1559.
(18) Greco, C.; Zampella, G.; Bertini, L.; Bruschi, M.; Fantucci, P.; De Gioia, L. *Inorg. Chem.* **2007**, *46*, 108−116. Greco, C.; Bruschi, M.; Fantucci, P.; De Gioia, L. *Eur. J. Inorg. Chem.* **2007**, *13*, 1835−1843. Hogarth, G.; Richards, I. *Inorg. Chem. Commun.* **2007**, *10*, 66−70. Gloaguen, F.; Lawrence, J. D.; Rauchfuss, T. B.; Benard, M.; Rohmer, M.-M. *Inorg. Chem.* **2002**, *41*, 6573−6582. Nehring, J. L.; Heinekey, D. M. *Inorg. Chem.* **2003**, *42*, 4288−4292.
(19) Noodleman, L.; Norman, J. G., Jr. *J. Chem. Phys.* **1979**, *70*, 4903−4906. Noodleman, L. *J. Chem. Phys.* **1981**, *74*, 5737−5743.
(20) Ryde, U. *J. Comput.-Aided Mol. Des.* **1996**, *10*, 153−164.
(21) Ryde, U.; Olsson, M. H. M. *Int. J. Quantum Chem.* **2001**, *81*, 335−374.
(22) Ahlrichs, R.; Bar, M.; Haser, M.; Horn, H.; Kolmel, C. *Chem. Phys. Lett.* **1989**, *162*, 165−169.
(23) Case, D.A. et al. *Amber 8*; University of California: San Francisco, CA, 2004.
(24) Cornell, W. D.; Cieplak, P. I.; Bayly, C. I.; Gould, I. R.; Merz, K. M.; Ferguson, D. M.; Spellmeyer, D. C.; Fox, T.; Caldwell, J. W.; Kolman, P. A. *J. Am. Chem. Soc.* **1995**, *117*, 5179−5197.

surrounding it, are included in system 3, which is kept fixed at the crystallographic coordinates. Apart from system 1, which is represented by a wave function during the QM/MM geometry optimizations, each atom is represented by a partial point charge, taken from the *Amber* libraries.[24] All such MM charges are included in the Hamiltonian of the QM calculations, and thus the quantum chemical system is polarized by the atoms of system 2 and 3 in a self-consistent way. When the quantum and classical regions are connected by a chemical bond, the link-atom approach is applied;[20,25] i.e., the QM system is truncated by hydrogen atoms, the positions of which are linearly related to the corresponding carbon atom in the protein.

The total QM/MM energy is calculated as

$$E_{\mathrm{QM/MM}} = E_{\mathrm{QM}} + E_{\mathrm{MM123}} - E_{\mathrm{MM1}} \quad (1)$$

Here, E_{QM} is the QM energy of the quantum system truncated by hydrogen atoms, including the interaction between system 1 and the surrounding point charges. E_{MM1} is the MM energy of the quantum system, still truncated by hydrogen atoms, but without any electrostatic interactions. Finally, E_{MM123} is the classical energy of all the atoms in the system with carbon atoms at the junctions and with the charges of the QM region zeroed, to avoid double counting of the electrostatic interactions. Such an approach, which is similar to the one used in the Oniom method,[26] should lead to the cancellation of errors caused by the truncation of the quantum system.

Geometry optimizations were carried out in three steps. First, systems 2 and 3 were frozen and only the quantum system was optimized (geometries obtained at the end of this optimization step will be referred to as Protein_Fixed). Second, both system 1 and system 2 were allowed to relax. In the MM optimization of system 2, the charges on the quantum atoms were updated after each iteration of the QM/MM optimization.[21] This optimization was performed with the looser convergence criterion of 10^{-4} a.u. for the change in energy and 10^{-2} a.u. for the maximum norm of the Cartesian gradient (0.26 kJ mol^{-1} and 50 kJ (mol Å)$^{-1}$). Then, system 2 was frozen again, and the geometry optimization was continued with default convergence criteria (10^{-6} and 10^{-3} a.u.). If not otherwise stated, the discussion is based on the results obtained with the protein portion included in system 2 free to relax, because these structures are expected to be more realistic.

2.2. The Protein. All QM/MM calculations were based on the 1.6 Å resolution structure of the Fe-only hydrogenase from *D. desulfuricans* (PDB code 1HFE).[6] This is a heterodimer composed of a large subunit that harbors the H-cluster and the two accessory Fe_4S_4 assemblies, and a small subunit. This crystal structure was selected because it has the highest resolution among the published Fe-only hydrogenase structures. Hydrogen atoms were added to the crystal structure, and the protein was solvated in a sphere of water molecules with a radius of 48 Å. To optimize the positions of hydrogen atoms and solvent water molecules, a 90 ps simulated-annealing molecular dynamics calculation was carried out, followed by 10 000 steps of conjugate gradient energy minimization. The protonation state of the histidine side chains was chosen by considering solvent exposure and a detailed study of the hydrogen-bond network around the residue; this means that, for each histidine side chain, all possible hydrogen-bond donors and acceptors in close proximity of the imidazole nitrogen atoms were identified, and a congruent disposition of proton(s) on the ring was then established. As a result of such a procedure, we assigned protonation of $N^{\delta 1}$ for residues S89 (the letter S indicates the small subunit; residue numbers without a S refer to the large subunit) and 75; protonation of $N^{\epsilon 2}$ for residues 351 and 371; and protonation on both the nitrogen atoms of the imidazole ring for residues S82, S85, S91, 14, 26, 58, 62, 141, and 196. All lysine and arginine residues were considered in their positively charged state, while aspartate and glutamate sidechains were always included in the anionic form. Finally, the iron-bound cysteine residues (i.e., amino acids 36, 38, 41, 45, 66, 69, 72, 76, 179, 234, 378, and 382) were assumed to be deprotonated. All the ligands found in the PDB file were included in the QM/MM model, except a water molecule bridging Fe_d and Fe_p, which was replaced by a carbonyl group, following a more recent correction[5b] of the crystal structure.[6]

As pointed out in the Introduction, the Fe-only hydrogenase from *D. desulfuricans* includes two accessory iron−sulfur clusters in addition to the H-cluster. For these Fe_4S_4 sites, we used Merz−Kollman electrostatic potential charges,[27] taken from QM calculations at the B3LYP/6-31G* level for truncated models of each site. One of the iron−sulfur clusters belongs to system 2 (i.e., the MM region that is free to relax), and thus, a set of MM parameters had to be also defined in this case. To this end, a QM frequency calculation was run, and force constants of all relevant bonds, angles, and dihedrals were extracted from the Hessian matrix, using the approach suggested by Seminario.[28] The accessory Fe_4S_4 clusters can reside in two alternative redox states. Following previous experimental results,[9a,c,e,f] we adopted the $[Fe_4S_4]^{2+}$ state for the $\mathbf{H_{ox}^{inact}}$ and $\mathbf{H_{ox}^{cat}}$ forms of the enzyme, while in the case of the reduced forms of the enzyme (models $\mathbf{HD^{3-}}$, $\mathbf{D^{3-}_{(H^-)}}$, and $\mathbf{D2^{3-}_{(H^-)}}$ in Figure 5), the $[Fe_4S_4]^{+}$ state was chosen. For the other intermediates in the catalytic cycle, QM/MM optimizations were carried out using both the +1 and +2 redox states.

2.3. Quantum Chemical Calculations. All QM calculations described in the present paper were carried out within the density functional theory (DFT) framework, using the BP86 functional[29] and an all-electron split-valence basis with polarization functions on all atoms (SVP).[30] Moreover, we applied the resolution of identity (RI) technique,[31,32] which sped up the calculations by a factor of ∼10. However, after all the QM/MM geometry optimizations carried out at the BP86/SVP-RI level, a single point calculation at the B3LYP/TZVP level was performed. In fact, the use of the hybrid functional B3LYP in conjunction with the large triple-ζ basis TZVP is expected to give more reliable QM energy values. In the present work, we report two different sets of QM/MM relative energies, i.e., with ($\Delta E_{\mathrm{totMM}}$) or without ($\Delta E_{\mathrm{tot}}$) the MM energy contributions resulting from the relaxation of system 2. The accuracy in energy calculations is estimated to be ∼25 and ∼40 kJ mol^{-1} for ΔE_{tot} and $\Delta E_{\mathrm{totMM}}$ values, respectively.

A theoretical investigation on the entire H-cluster is a challenge because the Fe_4S_4 cluster is composed of two Fe_2S_2 layers of high-

(25) Reuter, N.; Dejaegere, A.; Maigret, B.; Karplus, M. *J. Phys. Chem.* **2000**, *104*, 1720−1735.

(26) Svensson, M.; Humbel, S.; Froese, R. D. J.; Matsubara, T.; Sieber, S.; Morokuma, K. *J. Phys. Chem.* **1996**, *100*, 19357−19363.

(27) Besler, B. H.; Merz, K. M.; Kollman, P. A. *J. Comput. Chem.* **1990**, *11*, 431.

(28) Seminario, J. M. *Int. J. Quantum Chem., Quant. Chem. Symp.* **1996**, *30*, 59−65. Nilsson, K.; Lecerof, D.; Sigfridsson, E.; Ryde, U. *Acta Crystallogr., Sect. D: Biol. Crystallogr.* **2003**, *59*, 274−289.

(29) Becke, A. D. *Phys. Rev. A: At., Mol., Opt. Phys.* **1988**, *38*, 3098−3100. Perdew, J. *Phys. Rev. B: Condens. Matter Mater. Phys.* **1986**, *33*, 8822−8824.

(30) Schaefer, A.; Horn, H.; Ahlrichs, R. *J. Chem. Phys.* **1992**, *97*, 2571−2574.

(31) Eichkorn, K.; Treutler, O.; Öhm, H.; Haser, M.; Ahlrichs, R. *Chem. Phys. Lett.* **1995**, *240*, 283−289.

(32) Eichkorn, K.; Weigend, F.; Treutler, O.; Ahlrichs, R. *Theor. Chim. Acta* **1997**, *97*, 119−124.

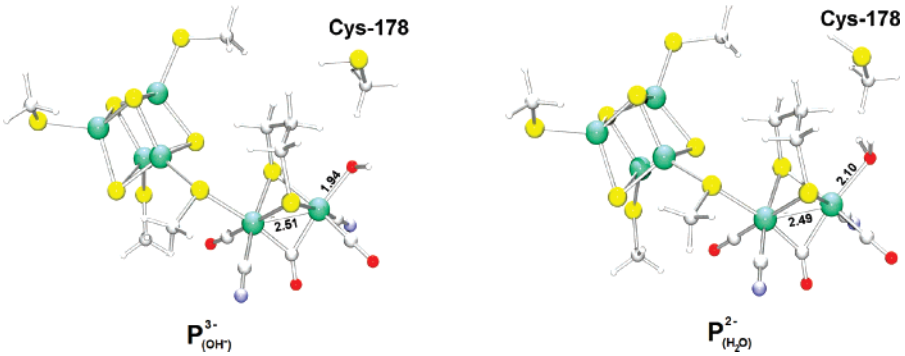

Figure 1. QM/MM optimized structures of the hydroxo- (left) and water-bound (right) $\mathbf{H_{ox}^{inact}}$ forms of the PDT-containing H cluster. Selected distances are given in Å.

spin Fe atoms coupled antiferromagnetically to give an overall low-spin ground state. The ground-state wave function of such spin-coupled systems corresponds to a linear combination of multiple determinants that cannot be treated within the single-determinant DFT approach. However, in the framework of the unrestricted formalism, these interactions can be modeled with the BS approach introduced by Noodleman and Norman, Jr.[19] The BS approach consists of the localization of opposite spins of the monodeterminant wave function in different parts of the molecule.

As noted by Brunold,[33] the Fe atoms of Fe_4S_4 are not equivalent in the H-cluster, and therefore, six different BS configurations can be generated for each species. However, we only considered one of the six possible BS wave function variants. In fact, various QM/MM and QM calculations on the reduced form of the enzyme (data not shown) have indicated that the structural differences among H-cluster models characterized by different BS configurations are very small (the differences between corresponding bond lengths in the Fe_2S_2 cluster were always below 0.02 Å), and the QM/MM energies never differed by more than 10 kJ mol^{-1}. We also validated the use of the BP86/SVP level of theory by carrying out BS QM/MM geometry optimizations on models of the $\mathbf{H_{ox}^{cat}}$ form of the enzyme, in the context of the BP86/TZVP level of theory. The use of the TZVP basis (a triple-ζ polarized basis set) gave place to structures very similar to the ones obtained at the BP86/SVP level (see the Supporting Information for details), thus supporting the computational approach used in the rest of our work.

2.4. Composition of the Model Systems. System 1, i.e., the QM system of the various Fe-only hydrogenase models here considered, always included the iron and sulfide ions of the Fe_6S_6 H-cluster, a PDT or a DTMA ligand bridging Fe_d and Fe_p, three CO groups, two cyanide ligands, and four CH_3S^- groups that represent the cysteine residues connecting the Fe_6S_6 cluster to the rest of the enzyme large subunit (Cys-179, Cys-234, Cys-378, Cys-382). In addition, the side chain of Cys-178 was also included in the QM region, in the form of a CH_3SH group. This residue is in close proximity to the bidentate ligand of the binuclear subcluster, and it might act as the terminal element of the proton channel that supplies protons to the H-cluster during the dihydrogen-evolving route.[5a]

The QM systems of the various QM/MM models considered in this paper differ in the composition of the Fe_d coordination sphere. The coordination site trans to the μ-CO group on Fe_d was either vacant or occupied by an exogenous ligand like H^-, H_2, OH^-, or H_2O. Finally, when a DTMA residue is present in the model, the two possible protonation states of its amine group were considered. The Fe_4S_4 subcluster was always modeled in the +2 state (antiferromagnetically coupled low-spin state). This gives a total of 57−60 atoms in system 1. System 2 consisted of 217 amino acids and 41 water molecules, whereas system 3 included the rest of the protein and water molecules (267 residues and 7044 water molecules).

3. Results and Discussion

Before discussing the results of our work, it is worth illustrating the details of the nomenclature that will be used in this paper for the various enzyme forms here investigated. Depending on the presence of PDT, DTMA, or protonated DTMA in the binuclear subsite, the models will be termed "**P**", "**D**", or "**HD**", respectively; a superscript will be added to each name, in order to specify the charge of the QM system. Finally, a subscript will be also present if the model includes an exogenous ligand (OH^-, H_2O, H^-, H_2) bound to or in proximity of the distal iron atom.

3.1. Investigation of the PDT-Containing $\mathbf{H_{ox}^{inact}}$ Form of the Enzyme and Its Activation Route. The nature of the $\mathbf{H_{ox}^{inact}}$ form of Fe-only hydrogenases has been a matter of recent debate. $Fe^{II}Fe^{II}$ binuclear subclusters in which either a water or a hydroxo ligand is terminally bound to Fe_d are good candidates for $\mathbf{H_{ox}^{inact}}$. In fact, X-ray diffraction data[5a,12] and some DFT studies[10] support this picture. However, a recent computational study suggests that a water molecule does not bind the diferrous Fe_2S_2 subsite in $\mathbf{H_{ox}^{inact}}$.[34] Moreover, despite insights obtained by theoretical and experimental works, crucial details about the transition from $\mathbf{H_{ox}^{inact}}$ to the mixed-valence $Fe^{II}Fe^{I}$ active state ($\mathbf{H_{ox}^{cat}}$) are missing.[10,11,34,35]

Investigation of the oxidized, inactive $\mathbf{H_{ox}^{inact}}$ form of the enzyme was started from an active-site model including as the chelating ligand a PDT group and formally corresponding to the $[2Fe^{II}2Fe^{III}]$ and $Fe^{II}Fe^{II}$ redox states for the Fe_4S_4 and $[2Fe]_H$ clusters, respectively.

In the $\mathbf{H_{ox}^{inact}}$ model containing a hydroxo group coordinated to Fe_d ($\mathbf{P^{3-}_{(OH^-)}}$; Figure 1), the Fe_d−O distance is 1.94 Å and the hydroxo group does not interact with the protein environment. Notably, protonation of the hydroxo group in $\mathbf{P^{3-}_{(OH^-)}}$ is extremely favorable (−220 kJ mol^{-1}, see Table

(33) Flieder, A. T.; Brunold, T. C. *Inorg. Chem.* **2005**, *44*, 9322−9334.

(34) Motiu, S.; Dogaru, D.; Gogonea, V. *Int. J. Quantum Chem.* **2007**, *107*, 1248−1252.

(35) Parkin, A.; Cavazza, C.; Fontecilla-Camps, J. C.; Armstrong, F. A. *J. Am. Chem. Soc.* **2006**, *128*, 16808−16815.

Table 1. Computed Reaction Energies for Isomerizations, Protonation,[a,b] and Water/Dihydrogen Binding[c]

reaction	ΔE_{totMM} (kJ mol^{-1})	ΔE_{tot} (kJ mol^{-1})
$\mathbf{P}^{2-}_{(H_2O)} \rightarrow \mathbf{P}^{2-} + H_2O$	+72	+78
$\mathbf{P}^{3-}_{(H_2O)} \rightarrow \mathbf{P}^{3-} + H_2O$	+29	−10
$\mathbf{P}^{3-}_{(OH^-)} + H^+ \rightarrow \mathbf{P}^{2-}_{(H_2O)}$	−220	−103
$\mathbf{P}^{4-}_{(OH^-)} + H^+ \rightarrow \mathbf{P}^{3-}_{(H_2O)}$	−440	−283
$\mathbf{D}^{2-}_{(H_2O)} \rightarrow \mathbf{D}^{2-} + H_2O$	+122	+107
$\mathbf{D}^{3-}_{(H_2O)} \rightarrow \mathbf{D}^{3-} + H_2O$	−40	+5
$\mathbf{D}^{3-}_{(OH^-)} + H^+ \rightarrow \mathbf{D}^{2-}_{(H_2O)}$	−209	−89
$\mathbf{D}^{4-}_{(OH^-)} + H^+ \rightarrow \mathbf{D}^{3-}_{(H_2O)}$	−419	−296
$\mathbf{HD}^{3-} \rightarrow \mathbf{D}^{3-}_{(H^-)}$	−44	−35
$\mathbf{D}^{3-}_{(H^-)} \rightarrow \mathbf{D2}^{3-}_{(H^-)}$	+52	+41
$\mathbf{HD}^{3-}_{(H^-)} \rightarrow \mathbf{D}^{3-}_{(H_2)}$	+10	−13
$\mathbf{HD}^{2-}_{(H^-)} \rightarrow \mathbf{D}^{2-} + H_2$	+167	+156
$\mathbf{D}^{3-}_{(H_2)} \rightarrow \mathbf{D}^{3-} + H_2$	−30	−14

[a] Energy values were obtained by considering the energy of a solvated proton to be −1098 kJ mol^{-1}.[37] [b] The relatively large discrepancies between ΔE_{totMM} and ΔE_{tot} for protonation reactions are due to the different charge of the QM system used to calculate such energy differences; the influence of charge variation in system 1 on the structure of system 2 can be accounted for only when the ΔE_{totMM} values are computed, while it is neglected when the ΔE_{tot} values are considered. [c] Water binding energies were obtained by considering as the reference a water molecule in a waterlike continuum solvent. To discuss water binding reactions, it was also necessary to compute the E_{totMM} and E_{tot} energies for models that did not include any water molecule in the QM region, i.e., model $\mathbf{D}^{3-}$ (see Figure 7) and models $\mathbf{P}^{2-}$, $\mathbf{P}^{3-}$, and $\mathbf{D}^{2-}$ (structures not shown). The energies associated with dihydrogen binding to models $\mathbf{D}^{3-}$ and $\mathbf{D}^{2-}$ were computed by considering as the reference a H_2 molecule in a waterlike continuum solvent.

1), indicating that this process is spontaneous in the protein. When a water molecule is bound to the bimetallic cluster, the Fe_d−O distance increases to 2.10 Å ($\mathbf{P}^{2-}_{(H_2O)}$; Figure 1). Moreover, the water binding energy in $\mathbf{P}^{2-}_{(H_2O)}$ is quite large (72 kJ mol^{-1}; energy value obtained considering as reference a water molecule in a waterlike continuum solvent), indicating that, even taking into account entropic effects (about 30 kJ mol^{-1}),[36] a water molecule is bound to Fe_d in the $\mathbf{H_{ox}}^{\mathbf{inact}}$ state.

It was previously proposed that one-electron reduction of the $\mathbf{H_{ox}}^{\mathbf{inact}}$ form of the enzyme could lead to the release of water from Fe_d, preparing the protein to bind its substrates (i.e., protons or molecular hydrogen).[10a] Interestingly, QM/MM optimization of a species ($\mathbf{P}^{3-}_{(H_2O)}$) obtained by adding one electron to the water-bound form of the enzyme $\mathbf{P}^{2-}_{(H_2O)}$ led to the release of the water molecule from Fe_d (Fe_d−O distance = 3.26 Å; Figure 2). Note that the released water molecule, even if not interacting directly with the H-cluster, remains in the active site and forms a hydrogen bond with Cys-178. This state may precede the definitive release of H_2O from the active-site cavity. In fact, the water binding energy to the protein in $\mathbf{P}^{3-}_{(H_2O)}$ is 29 kJ mol^{-1} (Table 1).

We have also investigated a $Fe^{II}Fe^{I}$ form in which a hydroxo group is terminally coordinated to Fe_d ($\mathbf{P}^{4-}_{(OH^-)}$; Figure 2). In $\mathbf{P}^{4-}_{(OH^-)}$, the Fe_d−O distance is 1.99 Å and the Fe−Fe distance is significantly longer than that in $\mathbf{P}^{3-}_{(OH^-)}$ and $\mathbf{P}^{3-}_{(H_2O)}$ (2.57 Å in $\mathbf{P}^{4-}_{(OH^-)}$; see Figure 2). The proton affinity of the OH^- group coordinated to Fe_d in $\mathbf{P}^{4-}_{(OH^-)}$ is extremely large (−440 kJ mol^{-1}; Table 1), indicating that protonation of the hydroxo group of the cluster is spontaneous on both the $Fe^{II}Fe^{I}$ and $Fe^{II}Fe^{II}$ species.

3.2. Investigation of the DTMA-Containing $\mathbf{H_{ox}}^{\mathbf{inact}}$ Form of the Enzyme and Its Activation Route. Next, we studied how the replacement of PDT with DTMA affects the $\mathbf{H_{ox}}^{\mathbf{inact}}$ form. Initially, a DTMA-containing $\mathbf{H_{ox}}^{\mathbf{inact}}$ form featuring a hydroxo group bound to Fe_d was investigated. Both the protonated and unprotonated forms of DTMA were considered. In the optimized geometry of the $\mathbf{H_{ox}}^{\mathbf{inact}}$ form featuring unprotonated DTMA ($\mathbf{D}^{3-}_{(OH^-)}$; Figure 3), the Fe_d−O distance is 1.97 Å and a hydrogen bond is formed between the NH group of DTMA and the oxygen atom of the hydroxo ligand; in turn, the lone pair of the nitrogen atom in DTMA establishes a hydrogen bond with the thiol group of Cys-178. QM/MM optimizations started from a model with a protonated DTMA and a hydroxo ligand coordinated to Fe_d always resulted in proton transfer from DTMA to the hydroxo group ($\mathbf{D}^{2-}_{(H_2O)}$; Figure 3). This result shows that there is no barrier for the proton-transfer process and indicates that the hydroxo group bound to Fe_d is more basic than DTMA. Thus, formation of a water molecule in the $\mathbf{H_{ox}}^{\mathbf{inact}}$ state, as a result of protonation of the corresponding hydroxo-bound group, can take place on a $Fe^{II}Fe^{II}$ binuclear subcluster also when the bidentate ligand includes an amine group.

The water molecule coordinated to Fe_d in $\mathbf{D}^{2-}_{(H_2O)}$ forms a hydrogen bond with the N atom of DTMA. The formation of this hydrogen bond is accompanied by the inversion of the NH group of DTMA (relative to $\mathbf{D}^{3-}_{(OH^-)}$) and the formation of a hydrogen bond also between the NH group of DTMA and the S atom of Cys-178 (Figure 3).

It should also be noted that the protonation of the OH^- group coordinated to Fe_d in $\mathbf{D}^{3-}_{(OH^-)}$ is thermodynamically favorable (Table 1), further supporting the suggestion[10a] that a water-bound form of the H-cluster can be involved in the activation of the enzyme from the catalytically inactive $\mathbf{H_{ox}}^{\mathbf{inact}}$ state to the active $\mathbf{H_{ox}}^{\mathbf{cat}}$ state.

A one-electron reduction of $\mathbf{D}^{3-}_{(OH^-)}$ and $\mathbf{D}^{2-}_{(H_2O)}$ leads to the $Fe^{II}Fe^{I}$ species $\mathbf{D}^{4-}_{(OH^-)}$ and $\mathbf{D}^{3-}_{(H_2O)}$, respectively. In the hydroxo-bound species $\mathbf{D}^{4-}_{(OH^-)}$, the Fe_d−O distance is 2.01 Å and the OH−NH−SH hydrogen-bond network is even stronger than that in $\mathbf{D}^{3-}_{(OH^-)}$, as deduced from the shortening of the relevant interatomic distances going from $\mathbf{D}^{3-}_{(OH^-)}$ to $\mathbf{D}^{4-}_{(OH^-)}$ (Figures 3 and 4).

A one-electron reduced Fe_6S_6 assembly showing a water molecule bound to Fe_d (model $\mathbf{D}^{3-}_{(H_2O)}$, Figure 4) corresponds to a minimum on the QM/MM PES of the DTMA-containing H-cluster. This is most likely due to the strong hydrogen bond (1.55 Å) between the water molecule and the amine group of DTMA; in fact, in the corresponding PDT-containing adduct $\mathbf{P}^{3-}_{(H_2O)}$, no hydrogen bonds between the water molecule and the H-cluster could be established, and as a result, the H_2O ligand detached from the partially oxidized cluster. However, water binding to the H-cluster is much weaker in the $\mathbf{H_{ox}}^{\mathbf{cat}}$ model $\mathbf{D}^{3-}_{(H_2O)}$ than in the oxidized $\mathbf{H_{ox}}^{\mathbf{inact}}$ model $\mathbf{D}^{2-}_{(H_2O)}$, as indicated by the 0.12 Å difference

(36) Amzel, L. M. *Proteins: Struct., Funct., Genet.* **1997**, *28*, 144−149. Rul'šek, L.; Jensen, K. P.; Lundgren, K.; Ryde, U. *J. Comput. Chem.* **2006**, *27*, 1398−1414.
(37) Klots, C. E. *J. Phys. Chem.* **1981**, *85*, 3585−3588. Topol I. A.; Tawa, G. J.; Burt, S. K.; Rashin, A. A. *J. Phys. Chem.* **1997**, *101*, 10075−10081.

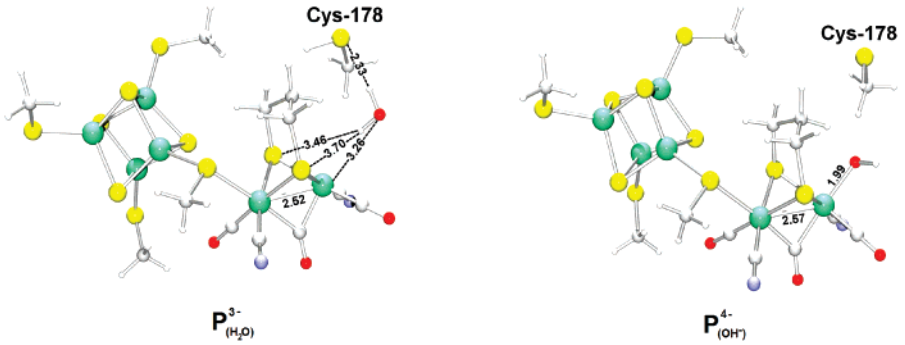

Figure 2. QM/MM optimized structures of the water-bound, partially oxidized forms of the PDT-containing H-cluster ($\mathbf{P^{3-}_{(H_2O)}}$; left) and the corresponding hydroxo-containing form of the active site ($\mathbf{P^{4-}_{(OH^-)}}$; right). Selected distances are given in Å.

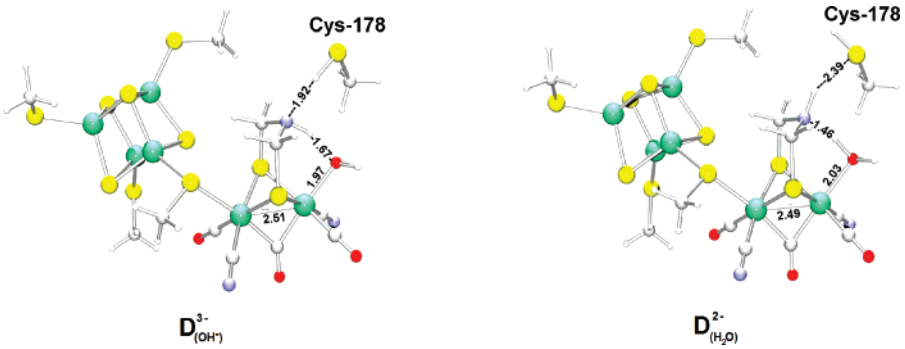

Figure 3. On the left: QM/MM optimized structures of the hydroxo-bound, completely oxidized ($\mathbf{H_{ox}^{inact}}$) form of the DTMA-containing H-cluster. On the right: the oxidized H-cluster structure resulting from the QM/MM optimization of a guess geometry characterized by a DTMA residue with a protonated amine group and a hydroxo group bound to Fe_d. Selected distances are given in Å.

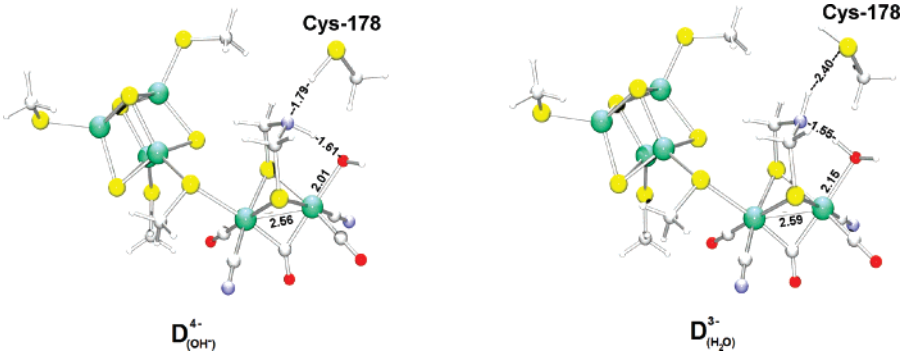

Figure 4. QM/MM optimized structures of the hydroxo-bound, partially oxidized form of the DTMA-containing H-cluster (on the left) and the corresponding water-containing form of the active site (on the right). Selected distances are given in Å.

in the Fe_d−O bond distances. The same conclusion can be drawn from the computed binding energies of the water molecules in $\mathbf{D^{2-}_{(H_2O)}}$ and $\mathbf{D^{3-}_{(H_2O)}}$ (122 and −40 kJ mol^{-1}, respectively).

3.3. Investigation of the Catalytic Cycle of Fe-Only Hydrogenase. Release of the water molecule in the $\mathbf{H_{ox}^{cat}}$ state of the protein leads to the formation of a vacant coordination site trans to the μ-CO group, where substrate binding could initiate the catalytic cycle. In particular, along the pathway to molecular hydrogen evolution, monoelectron reduction of $\mathbf{H_{ox}^{cat}}$ leads to a [2Fe^{II}2Fe^{III}], Fe^{I}Fe^{I} species, which should correspond to the experimentally characterized $\mathbf{H_{red}}$ form. In fact, previous results obtained on binuclear models suggested that a proton can bind to the Fe^{I}Fe^{I} form of the binuclear subsite, and protonated DTMA could represent a convenient source of protons for the hydrogen-evolving path (Scheme 3).[10b,14,15]

Prompted by the above observations, as a first step of the investigation of Fe-only hydrogenase catalytic cycle, we carried out the optimization of two different forms of the enzyme in which the overall charge of the H-cluster is −3. In the first, which formally corresponds to a [2Fe^{II}2Fe^{III}], Fe^{I}Fe^{I} redox state, DTMA is protonated and a coordination site on Fe_d is vacant (Scheme 3, Figure 5, model $\mathbf{HD^{3-}}$); in the second, a proton has moved from DTMA to Fe_d, thus giving rise to a formal Fe^{II}Fe^{II} subcluster with a terminal hydride ligand (model $\mathbf{D^{3-}_{(H^-)}}$; Figure 5).

Evaluation of QM/MM energies indicates that the hydride form $\mathbf{D^{3-}_{(H^-)}}$ is 44 kJ mol^{-1} more stable than $\mathbf{HD^{3-}}$, suggesting that the crystallographic structure of the $\mathbf{H_{red}}$ form of DdH determined by Nicolet et al.[5b] could correspond to a hydride-bound form of the H-cluster. Comparison of computed and experimental structures (the structure of the $\mathbf{H_{red}}$ form is not available in the PDB, and only the distances

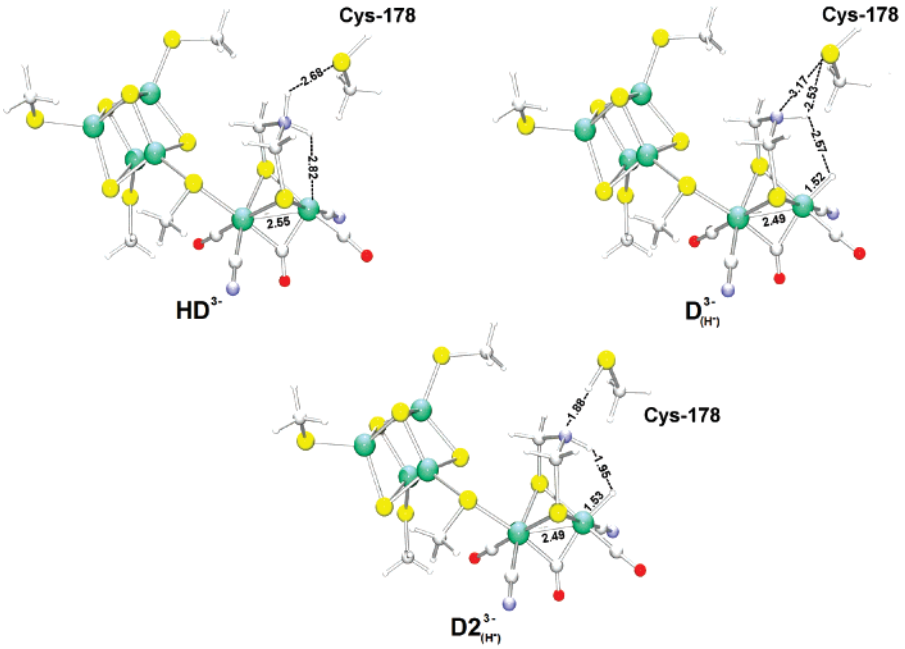

Figure 5. QM/MM optimized structures of a $Fe^{I}Fe^{I}$ form of the H-cluster featuring a vacant coordination site on Fe_d ($\mathbf{HD}^{3-}$) and of the corresponding hydride-bound isomers ($\mathbf{D}^{3-}_{(H^-)}$ and $\mathbf{D2}^{3-}_{(H^-)}$). Selected distances are given in Å.

Table 2. Comparison between the Available Experimental Interatomic Distances for the Reduced Form of the Enzyme[5b] and the Corresponding Computed Values for the QM/MM Geometries of $\mathbf{D}^{3-}_{(H^-)}$ and $\mathbf{P}^{3-}_{(H^-)}$

distance considered	computed bond lengths for complex $\mathbf{D}^{3-}_{(H^-)}$ (Å)	computed bond lengths for complex $\mathbf{P}^{3-}_{(H^-)}$ (Å)	experimental bond lengths[5b] in the two independent molecules (Å)
Fe_p-Fe_d	2.49	2.49	2.55; 2.61
$Fe_p-C(\mu\text{-CO})$	2.01	2.01	2.40; 2.56
$Fe_d-C(\mu\text{-CO})$	1.89	1.89	1.69; 1.69
$Fe_p-O(\mu\text{-CO})$	2.99	3.00	2.91; 3.12
$Fe_d-O(\mu\text{-CO})$	2.91	2.91	2.80; 2.80
N(DTMA)/C(PDT)−S(Cys-178)	3.17	3.37	3.1[a]

[a] On the basis of the crystal structure of the reduced DdH obtained by Nicolet and co-workers, it is not possible to distinguish between the presence of a PDT or DTMA ligand in the Fe_2S_2 subcluster;[5b] thus, in the present table, the interatomic distance between the central atom of the chelating ligand and the sulfur atom in Cys-178 is indifferently attributed to the "N(DTMA)−S(Cys-178)" and "C(PDT)−S(Cys-178)" pairs of atoms.

collected in Table 2 are given in the original publication[5b]) shows a reasonable agreement, keeping in mind that protein crystals at 1.85 Å resolution (such as the structure of $\mathbf{H}_{red}$) typically exhibit errors in bond distances of about 0.1 Å and errors of up to 0.3 Å are frequently observed[38,39] (indeed, the two independent molecules in the crystal show differences of 0−0.21 Å in the reported distances). The only significant discrepancy between the computed and experimental $\mathbf{H}_{red}$ structures is the position of the semibridging CO molecule; in particular, the difference between the computed and experimental Fe_p-C distances is as large as 0.37−0.53 Å. Such a large difference stems from the flatness of the energy landscape associated to the movement of the semibridging CO. In fact, in vacuum geometry optimizations with the Fe_p-C distance constrained to either the experimental or the QM/MM computed values resulted in an energy difference of less than 5 kJ mol^{-1}.

With the aim of shedding light on the nature of the chelating moiety in the binuclear cluster (PDT vs DTMA), we have also optimized the PDT-containing version of $\mathbf{D}^{3-}_{(H^-)}$ ($\mathbf{P}^{3-}_{(H^-)}$, structure not shown); as summarized in Table 2, the comparison between the experimental and computational interatomic distances evidenced that $\mathbf{P}^{3-}_{(H^-)}$ is also compatible with the crystal structure of the reduced enzyme (see Table 2). However, the distance between the central atom of the chelating moiety and the sulfur atom of Cys-178 is better reproduced when DTMA is included in the binuclear subsite. This result supports the previous observations by Nicolet et al.,[5b] who pointed out that a 3.1 Å distance between the central atom of the dithiolate ligand and the Sγ of Cys-178 is indicative of the presence of a DTMA residue in the H-cluster.

The QM/MM calculations also disclosed key details of the catalytic cycle. In fact, the proton transfer from DTMA to Fe_d is concomitant with the inversion of the amine group of DTMA ($\mathbf{HD}^{3-} \rightarrow \mathbf{D}^{3-}_{(H^-)}$; Figure 5), a rearrangement that was not observed in corresponding QM calculations without the MM part in the model (not shown). The inversion leads to a structure of $\mathbf{D}^{3-}_{(H^-)}$ in which the remaining amine group of DTMA forms a weak hydrogen bond with the sulfur atom of Cys-178 and with the hydride coordinated to Fe_d. Notably,

(38) Ryde, U.; Nilsson, K. *J. Mol. Struct. (THEOCHEM)* **2003**, *632*, 259−275.
(39) Ryde, U.; Nilsson, K. *J. Am. Chem. Soc.* **2003**, *125*, 14232−14233.

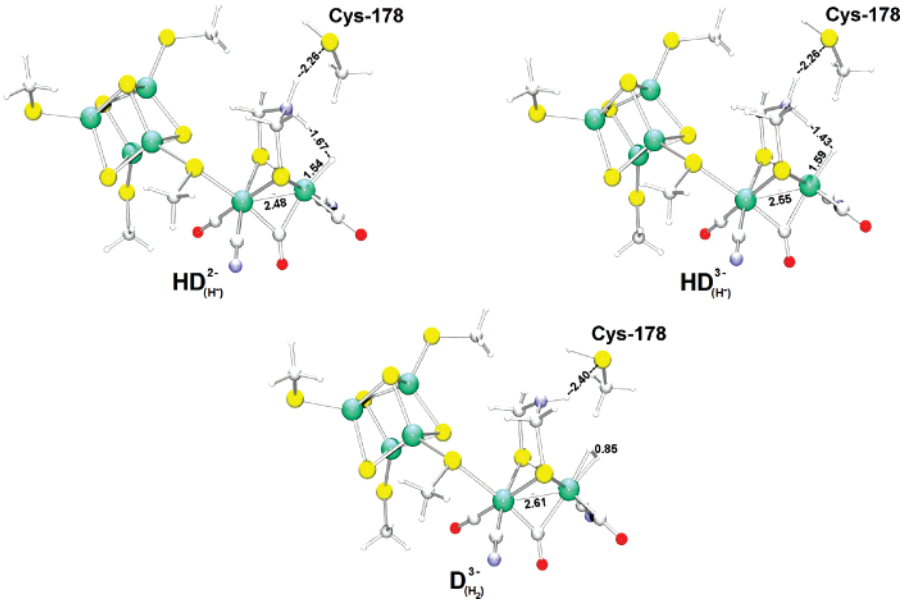

Figure 6. QM/MM optimized structures of the $\mathbf{HD}^{2-}_{(H^-)}$, $\mathbf{HD}^{3-}_{(H^-)}$, and $\mathbf{D}^{3-}_{(H_2)}$ intermediates of the catalytic cycle. Selected distances are given in Å.

a species where the side chain of Cys-178 (which has been proposed to act as the terminal element of the proton channel to the H-cluster[5a]) forms a hydrogen bond with the DTMA nitrogen atom ($\mathbf{D2}^{3-}_{(H^-)}$; Figure 5) is 52 kJ mol^{-1} less stable than $\mathbf{D}^{3-}_{(H^-)}$. Noteworthy, in $\mathbf{D2}^{3-}_{(H^-)}$, the NH group of DTMA strongly interacts with the terminal hydride group (H−H distance = 1.95 Å).

The next step in the catalytic cycle would be the protonation of the DTMA ligand in the hydride-bound H-cluster, leading to the intermediate species $\mathbf{HD}^{2-}_{(H^-)}$ (Scheme 3; Figure 6),[40] which could be in equilibrium with a species showing a H_2 molecule nonclassically bound to Fe_d, and a deprotonated DTMA residue.[14,15]

Such an equilibrium would correspond to the crucial step for catalysis, i.e., dihydrogen formation/splitting. However, a H_2 bound, [2Fe^{II}2Fe^{III}], Fe^{II}Fe^{II} species does not correspond to an energy minimum on the QM/MM potential energy surface: in fact, optimizations carried out starting from different plausible starting structures converged to $\mathbf{HD}^{2-}_{(H^-)}$. This result is relevant because it suggests that dihydrogen formation occurs on a form of the binuclear subsite more reduced than $\mathbf{HD}^{2-}_{(H^-)}$. This is also confirmed by the computation of the QM/MM energy associated with the formation and release of H_2 from $\mathbf{HD}^{2-}_{(H^-)}$, which is as large as 167 kJ mol^{-1} (see Table 1).

Monoelectronic reduction of $\mathbf{HD}^{2-}_{(H^-)}$ gave rise to $\mathbf{HD}^{3-}_{(H^-)}$ (Figure 6), an adduct characterized by a strong hydrogen bond between the Fe_d-bound hydride and the protonated amine group of DTMA.

Proton transfer from DTMA to Fe_d would then trigger H_2 formation (adduct $\mathbf{D}^{3-}_{(H_2)}$, Figure 6); $\mathbf{D}^{3-}_{(H_2)}$ is only 10 kJ mol^{-1} less stable than $\mathbf{HD}^{3-}_{(H^-)}$. Moreover, results from restrained optimizations along the proton-transfer path

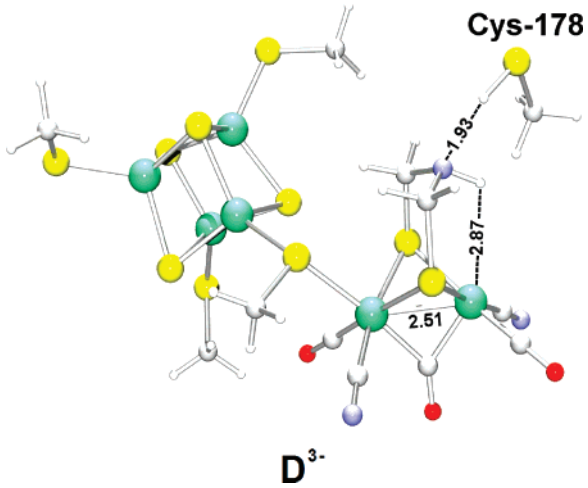

Figure 7. QM/MM optimized structure of model $\mathbf{D}^{3-}$. Selected distances are given in Å.

indicate that dihydrogen formation is associated with a low-energy barrier of 35 kJ mol^{-1}. Noteworthy, the inversion of the DTMA amine group was observed during the optimization of $\mathbf{D}^{3-}_{(H_2)}$; analogously to the case of $\mathbf{D}^{3-}_{(H^-)}$, this rearrangement was not observed in corresponding QM calculations without the MM part in the model (not shown). The relative position of Cys-178 with respect to the binuclear subsite (see Figure 6) suggests that the inversion of the amine group in DTMA could facilitate the protonation step that prepares the enzyme for a new catalytic cycle.

To close the catalytic cycle, H_2 must dissociate from $\mathbf{D}^{3-}_{(H_2)}$, giving rise to $\mathbf{D}^{3-}$, which corresponds to the Fe^{II}Fe^{I} $\mathbf{H}_{ox}^{cat}$ form of the enzyme (Figure 7). The H_2 binding energy to model $\mathbf{D}^{3-}$ turned out to be endothermic by 30 kJ mol^{-1}, indicating that H_2 release from a Fe^{II}Fe^{I} species is spontaneous, in good agreement with previous QM results.[15]

4. Conclusions

In the present work, a QM/MM investigation of the activation and catalytic mechanism of the *D. desulfuricans*

(40) All the structures reported in Figure 6 were obtained by QM/MM optimizations of enzyme models in which both the additional Fe_4S_4 clusters had a +2 redox state. Analogous QM/MM optimisations with a +1 redox state for these clusters gave essentially identical structures.

Scheme 4. Enzyme Activation and Catalytic Mechanism for Fe-Only Hydrogenases[a]

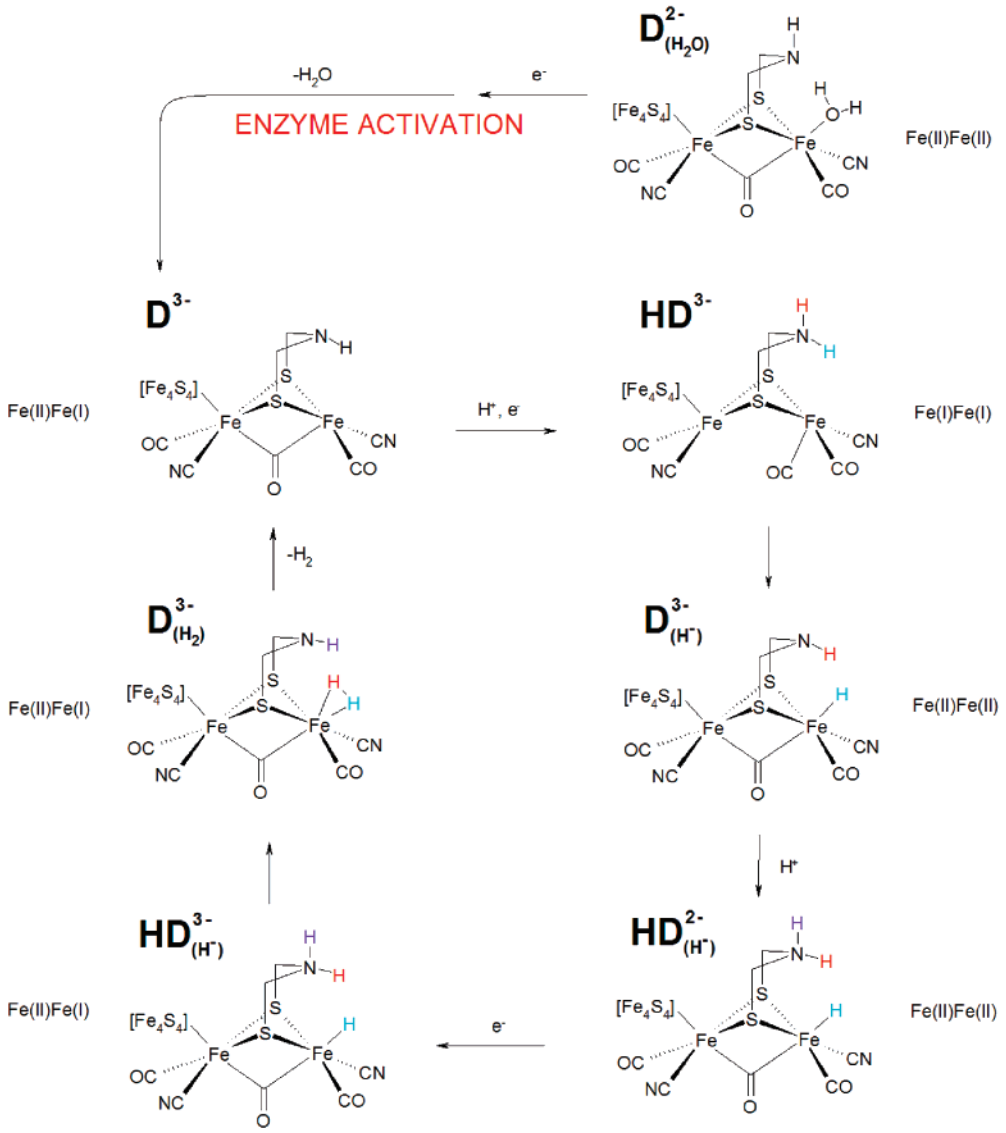

[a] As deduced from QM/MM calculations reported in the present paper. The names labeling the various models are assigned according to those appearing in Figures 3, 5, 6, and 7.

Fe-only hydrogenase is presented. Our results show that a hydroxo group bound to Fe_d in $\mathbf{H_{ox}^{inact}}$ is more basic than the DTMA ligand, and its conversion into a water molecule by means of a protonation step is facile. Moreover, the structural insights provided in the present work are useful to rationalize the experimental data recently published by Armstrong et al.[35] On the basis of their electrochemical experiments, they were not able to exclude that the acid version of a DTMA-containing, oxidized H-cluster could correspond to a hydroxo-bound active site bearing a protonated DTMA moiety. However, our data show that such a form of the enzyme would be unstable with respect to proton transfer from the protonated DTMA to the hydroxo group, thus supporting the alternative hypothesis that the acid form of the $\mathbf{H_{ox}^{inact}}$ active site is water-bound.

One-electron reduction of a water-bound $Fe^{II}Fe^{II}$ binuclear subsite including a bridging PDT ligand leads to the release of the water molecule from the H-cluster. The analogous step of one-electron reduction of a DTMA-containing H-cluster leads to the weakening of the interaction between the distal iron of the subcluster and the water oxygen atom, but the water molecule remains bound to Fe_d, because it forms a hydrogen bond with the amine group of DTMA. However, it is likely that it would dissociate, since this water-bound adduct corresponds to a local minimum on the QM/MM PES and the dissociation of the water molecule is energetically favorable ($\Delta E_{totMM} = -40$ kJ mol^{-1}; see also Scheme 4).

Our QM/MM investigation of the catalytic cycle indicates that the formation of H_2 from a species with terminal coordination of H to Fe_d ($\mathbf{HD^{3-}_{(H^-)}} \rightarrow \mathbf{D^{3-}_{(H_2)}}$, see Figure 6) is reversible with a small barrier.

A comparison between the DFT calculations carried out in a vacuum or in a continuum solvent model and the QM/MM results presented here allows us to show that the protein environment plays a subtle role in modulating the thermodynamic profile of the catalytic cycle as well as the geometric properties of key intermediates in the enzymatic process.

The calculation of the QM/MM energy difference associated with the first proton-transfer reaction ($\mathbf{HD^{3-}} \rightarrow \mathbf{D^{3-}_{(H^-)}}$, see Figure 5) indicates that the hydride form is 44 kJ mol^{-1} more stable than $\mathbf{HD^{3-}}$; notably, a very similar energy value for the same reaction (40 kJ mol^{-1}) was obtained by Zampella and co-workers through DFT optimizations carried out in a polarizable continuum medium with a dielectric constant of 4.[15] It is also important to emphasize the point that dihydrogen formation in the QM/MM model can take place only on the $Fe^{II}Fe^{I}$ form of the H-cluster, while H_2 evolution from a $Fe^{II}Fe^{II}$ form of the binuclear subsite is energetically hindered. Moreover, a H_2 molecule cannot remain nonclassically bound to the enzyme active site in the $Fe^{II}Fe^{II}$ redox state, because it would immediately undergo a heterolytic splitting process (see Figure 6, adduct $\mathbf{HD^{2-}_{(H^-)}}$). The outcome of these results in mechanistic terms is summarized in Scheme 4. The comparison between the latter scheme and Scheme 3 provides evidence for how the differences between the QM/MM results and previous DFT data are not limited to the details of the H_2 splitting/formation step; in fact, we also observed an inversion of the proton of the amine group in DTMA during the optimization of $\mathbf{D^{3-}_{(H^-)}}$ and $\mathbf{D^{3-}_{(H_2)}}$ (Figures 5 and 6 and Scheme 4). This suggests that the interplay between the H-cluster and its protein environment could have a functional relevance in the catalytic H_2 evolution, provided that the bidentate ligand that bridges the iron atoms in the binuclear subsite is actually a DTMA residue.

Supporting Information Available: Details related to the validation of the computational approach and the *Amber* parameter file used for the modeling of Fe_4S_4 cubanes at the MM level. This material is available free of charge via the Internet at http://pubs.acs.org.

IC062320A